Evaluation of Copper-64 Labeled AmBaSar Conjugated Cyclic RGD Peptide for Improved MicroPET Imaging of Integrin alpha(v)beta(3) Expression

ARTICLE *in* BIOCONJUGATE CHEMISTRY · AUGUST 2010

Impact Factor: 4.51 · DOI: 10.1021/bc900537f · Source: PubMed

7 AUTHORS, INCLUDING:

Hancheng Cai
University of Texas Southwestern Medical …
21 PUBLICATIONS **373** CITATIONS
SEE PROFILE

Zibo Li
University of North Carolina at Chapel Hill
116 PUBLICATIONS **4,248** CITATIONS
SEE PROFILE

chiun-wei Huang
University of Southern California
13 PUBLICATIONS **293** CITATIONS
SEE PROFILE

Peter S Conti
University of Southern California
261 PUBLICATIONS **7,217** CITATIONS
SEE PROFILE

Evaluation of Copper-64 Labeled AmBaSar Conjugated Cyclic RGD Peptide for Improved MicroPET Imaging of Integrin $\alpha_v\beta_3$ Expression

Hancheng Cai, Zibo Li, Chiun-Wei Huang, Anthony H. Shahinian, Hui Wang, Ryan Park, and Peter S. Conti*

Molecular Imaging Center, Keck School of Medicine, University of Southern California, Los Angeles, California 90033.
Received December 5, 2009; Revised Manuscript Received July 13, 2010

Recently, we have developed a new cage-like bifunctional chelator 4-((8-amino-3,6,10,13,16,19-hexaazabicyclo [6.6.6] icosane-1-ylamino) methyl) benzoic acid (AmBaSar) for copper-64 labeling and synthesized the positron emission tomography (PET) tracer ^{64}Cu-AmBaSar-RGD. In this study, we further evaluate the biological property of this new AmBaSar chelator by using ^{64}Cu-AmBaSar-RGD as the model compound. *In vitro* and *in vivo* stability, lipophilicity, cell binding and uptake, microPET imaging, receptor blocking experiments, and biodistribution studies of ^{64}Cu-AmBaSar-RGD were investigated, and the results were directly compared with the established radiotracer ^{64}Cu-DOTA-RGD. The ^{64}Cu-AmBaSar-RGD was obtained with high radiochemical yield (≥95%) and purity (≥99%) under mild conditions (pH 5.0−5.5 and 23−37 °C) in less than 30 min. For *in vitro* studies, the radiochemical purity of ^{64}Cu-AmBaSar-RGD was more than 97% in PBS or FBS and 95% in mouse serum after 24 h of incubation. The log *P* value of ^{64}Cu-AmBaSar-RGD was −2.44 ± 0.12. For *in vivo* studies, ^{64}Cu-AmBaSar-RGD and ^{64}Cu-DOTA-RGD have demonstrated comparable tumor uptake at selected time points on the basis of microPET imaging. The integrin $\alpha_v\beta_3$ receptor specificity was confirmed by blocking experiments for both tracers. Compared with ^{64}Cu-DOTA-RGD, ^{64}Cu-AmBaSar-RGD demonstrated much lower liver accumulation in both microPET imaging and biodistribution studies. Metabolic studies also directly supported the observation that ^{64}Cu-AmBaSar-RGD was more stable *in vivo* than ^{64}Cu-DOTA-RGD. In summary, the *in vitro* and *in vivo* evaluations of the ^{64}Cu-AmBaSar-RGD have demonstrated its improved Cu-chelation stability compared with that of the established tracer ^{64}Cu-DOTA-RGD. The AmBaSar chelator will also have general applications for ^{64}Cu labeling of various bioactive molecules in high radiochemical yield and high *in vivo* stability.

INTRODUCTION

The advancement of molecular imaging based on positron emission tomography (PET) is mainly driven by the discovery of imaging biomarkers and targeted molecules labeled with positron emitting radioisotopes (*1*−*3*). PET tracers have been widely applied in molecular imaging as these agents exhibit high binding affinity toward various promising biological targets, such as receptors or enzymes expressed during different phases of tumor growth or in other uncontrolled diseases (*3, 4*). Targeted copper-64 labeled molecules have shown promise for diagnostic PET imaging, as well as for radiotherapy, due to the favorable nuclear characteristics of the isotope ($t_{1/2}$ = 12.7 h, β^+ 17.4%, E_{max} = 0.656 MeV, β^- 39%, E_{max} = 0.573 MeV) and its availability with high specific activity (*5*). The half-life of ^{64}Cu is more suitable for developing biomolecule-based PET tracers, which usually require longer circulation times to achieve optimal targeting and uptake. Furthermore, ^{64}Cu-based PET tracers may be used to provide *in vivo* pharmacokinetic profiles of radiopharmaceuticals which contain the therapeutic radionuclide copper-67 ($t_{1/2}$ = 61.5 h, β^- 100%, E_{max} =0.121 MeV) (*6*). *In vivo* stable attachment of $^{64}Cu^{2+}$ to targeted biomolecules requires the use of a bifunctional chelator (BFC) (*7*). More and more ligands have been investigated as BFCs to complex $^{64}Cu^{2+}$ due to the development of copper coordination chemistry. Three of the most common chelators for $^{64}Cu^{2+}$ labeling are the macrocyclic ligands 1,4,7,10-tetraazacyclododecane-*N*,*N*′,*N*″,*N*‴-tetraacetic acid (DOTA), 1,4,8,11-tetraazacyclotetradecane-*N*,*N*′,*N*″,*N*‴-tetraacetic acid (TETA), and cross-bridged TETA ligands (*2, 5, 7, 8*). It is well known that DOTA, TETA, and their derivatives for $^{64}Cu^{2+}$ labeling have limited stability *in vivo* due to the dissociation of $^{64}Cu^{2+}$ from these BFCs, leading to high retention in the liver. A class of cross-bridged TETA derivatives has been developed that form stable complexes with $^{64}Cu^{2+}$ and are less susceptible to *in vivo* transchelation than their nonbridged TETA analogues (*9*). However, harsh $^{64}Cu^{2+}$ radiolabeling conditions (e.g., incubation at 85 °C under basic conditions) for cross-bridged TETA derivatives may result in the denaturation and hydrolysis of some biomolecules (*10*). Recently, a new class of bifunctional chelators has been synthesized on the basis of the sarcophagine (3,6,10,13,16,19-hexaazabicyclo [6.6.6] icosane, also called Sar) for $^{64}Cu^{2+}$ radiolabeling, resulting in extraordinarily stable ^{64}Cu-Sar based complexes *in vitro* and *in vivo* under physiological conditions (*11, 12*). The carboxylate and amino derivatives of the diamSar have also been developed by our group and Smith's group, respectively (*13*−*16*). These derivatives allow them to be readily cross-linked to amine or carboxyl residues on peptides and antibody molecules through amide bonds, yielding PET probes with improved pharmacokinetics, and dynamics due to the increased stability (*1, 15*).

The integrin $\alpha_v\beta_3$ receptor has been the attractive target of intensive research given its major role in several distinct processes, such as tumor angiogenesis and metastasis, and osteoclast mediated bone resorption (*17, 18*). The molecular imaging of integrin $\alpha_v\beta_3$ expression will allow the detection of cancer and other angiogenesis related diseases, patient stratification, and treatment monitoring of antiangiogenesis based therapy (*19, 20*). Although we and others have successfully developed various DOTA conjugated RGD peptides for multimodality imaging of integrin $\alpha_v\beta_3$ expression (*19*−*23*), the loss of ^{64}Cu from the chelator has led to unfavorable high

* To whom correspondence should be addressed. E-mail: pconti@usc.edu.

10.1021/bc900537f
Published on Web 07/28/2010

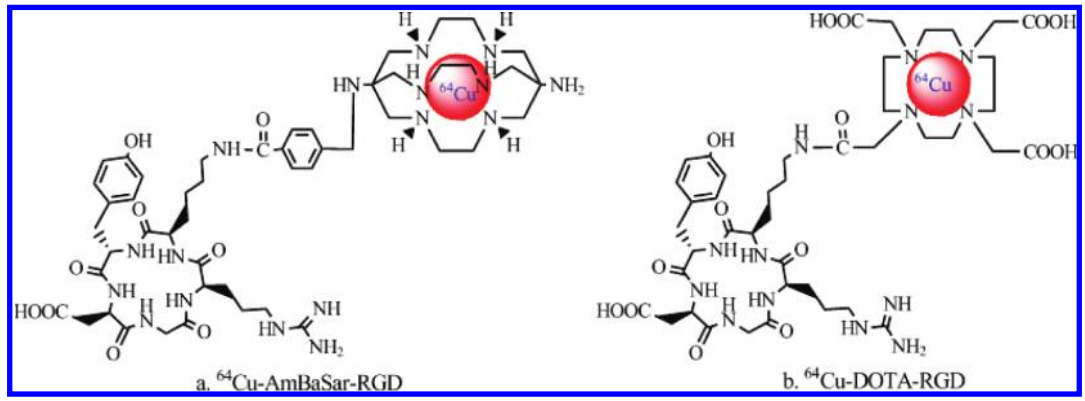

Figure 1. Chemical structures of ^{64}Cu-AmBaSar-RGD and ^{64}Cu-DOTA-RGD.

retention in the liver, resulting in high background. Therefore, the choice of a more stable BFC is preferred. As we mentioned above, we have developed a carboxylate derivative of diamSar, 4-((8-amino-3,6,10,13,16,19-hexaazabicyclo [6.6.6] icosane-1-ylamino) methyl) benzoic acid (AmBaSar) (*15, 16*), which could be conjugated to the primary amines in biomolecules through amide bonds. We also reported the synthesis of a new PET tracer ^{64}Cu-AmBaSar-RGD (Figure 1a). In this study, we further evaluated the conjugation and labeling conditions of ^{64}Cu-AmBaSar-RGD. Moreover, the *in vitro* and *in vivo* stability, lipophilicity, cell uptake, microPET imaging, and biodistribution studies of ^{64}Cu-AmBaSar-RGD and the established ^{64}Cu-DOTA-RGD (Figure 1b) were investigated to obtain a direct comparison of the two agents.

EXPERIMENTAL PROCEDURES

General. All reagents and solvents were purchased from Sigma-Aldrich Chemicals (St. Louis, MO, USA) and used without further purification unless otherwise stated. *N*,*N*-Diisopropylethylamine (DIPEA), 1-hydroxy-7-azabenzotriazole (HOAt), *O*-(7-azabenzotriazol-1-yl)-1,1,3,3-tetramethyluronium hexafluorophosphate (HATU), and Chelex 100 resin (50−100 mesh) were obtained from the Sigma-Aldrich Chemical Co. The c(RGDyK) peptide was purchased from Peptides International, Inc. (Louisville, KY, USA). DOTA was purchased from Macrocyclics (Dallas, TX, USA). The chelator AmBaSar was prepared following a method developed in our laboratory (*16*). $^{64}CuCl_2$ solution was ordered from University of Wisconsin (Madison, WI) or Washington University School of Medicine (St. Louis, MO), which both were produced through the ^{64}Ni(p,n)^{64}Cu nuclear reaction. Water was purified using a Milli-Q ultrapure water system from Millipore (Milford, MA, USA), followed by passing through a Chelex 100 resin before bioconjugation and radiolabeling.

Analytic and semipreparative reversed phase high performance liquid chromatography (HPLC) were accomplished on two Waters 515 HPLC pumps, a Waters 2487 absorbance UV detector, and a Ludlum Model 2200 radioactivity detector, which were operated by Waters Empower 2 software. The purification of AmBaSar, DOTA conjugated c(RGDyK) peptides, and ^{64}Cu-labeled peptides were performed on a Phenomenex Luna C18 reversed phase column (5 μm, 250 × 10 mm). The flow rate was 3 mL/min for semipreparative HPLC, with the mobile phase starting from 98% solvent A (0.1% TFA in water) and 2% solvent B (0.1% TFA in acetonitrile) (0−2 min) to 60% solvent A and 40% solvent B at 40 min. The separation was monitored using a radiodetector and UV at 218 and 254 nm. The analytic HPLC was performed with the same mobile phase gradient system and detection, except that a Phenomenex Luna C18 reversed phase analytic column (5 μm, 250 × 4.6 mm) was used at a flow rate of 1 mL/min. For the *in vivo* stability study, analytical HPLC was operated at the same conditions with a Rainin Microsorb-MV C18 column (5 μm, 250 × 4.6 mm) and the mobile phase starting from 98% solvent A and 2% solvent B (0−2 min) to 50% solvent A and 50% solvent B at 25 min. Radio-TLC was performed on MKC18 silica gel 60 Å plates (Whatman, NJ) with MeOH/20% NaOAc = 3:1 as the eluent. The plates were read with a Bioscan AR2000 imaging scanner (Washington, DC) and Winscan 2.2 software. Mass spectrometry using LC-MS was operated by the Proteomics Core Facility of the USC School of Pharmacy.

Syntheses of AmBaSar-RGD and DOTA-RGD. AmBaSar could be activated and conjugated to the c(RGDyK) peptide in a water-soluble procedure as reported earlier (*15*). The conjugation can also be performed in organic phase according to literature procedures (*24, 25*). Briefly, the solution of AmBaSar (4.5 mg, 0.01 mmol), HATU (3.8 mg, 0.01 mmol), HOAt (1.4 mg, 0.01 mmol), and dimethyl sulfoxide (DMSO, 0.5 mL) were stirred at room temperature for 10 min. Seven equivalents of DIPEA (9.1 mg, 0.07 mmol) and c(RGDyK) (1.2 mg, 0.002 mmol) in 300 μL of DMSO were then added to the mixture at 0 °C. The mixture was stirred for 3 h at room temperature, and the solvent removed *in vacuo*. The residue was dissolved in acetonitrile/water (1:3) containing 0.1% TFA and purified by semipreparative HPLC. AmBaSar-RGD was obtained as a white solid material after lyophilization. DOTA was activated and conjugated to c(RGDyK) as reported earlier (*23*). DOTA-RGD was also purified by semipreparative HPLC and confirmed by mass spectrometry. AmBaSar-RGD and DOTA-RGD conjugates were dissolved in 0.1 N ammonium acetate buffer solution (pH 5−5.5) and stored at −20 °C for future use in radiolabeling reactions.

Copper-64 Labeling and Formulation. The ^{64}Cu-AmBaSar-RGD was prepared using a method developed in our laboratory (*15*) with minor modifications as follows: [^{64}Cu]Acetate ($^{64}Cu(OAc)_2$) was prepared by adding 37−111 MBq of $^{64}CuCl_2$ in 0.1 N HCl into 300 μL of 0.1 N ammonium acetate buffer (pH 5.0−5.5), followed by mixing and incubating for 15 min at room temperature. The AmBaSar-RGD (about 2−5 μg in 100 μL 0.1 N ammonium acetate buffer) was added to the above $^{64}Cu(OAc)_2$ solution. The resulting mixture was incubated at a temperature of 23−37 °C for 30 min. The ^{64}Cu-AmBaSar-RGD was determined and purified by semipreparative HPLC. The radioactive peak containing ^{64}Cu-AmBaSar-RGD was collected and concentrated by rotary evaporation to remove organic solvent, and the radioactivity was reconstituted in 500−800 μL of phosphate buffered saline (PBS) and passed through a 0.22 μm Millipore filter into a sterile dose vial for use in the experiments below.

Details of the ^{64}Cu-labeling DOTA-RGD procedure were reported earlier (*23*). Briefly, 37−111 MBq of $^{64}CuCl_2$ in 0.1 N HCl was diluted in 300 μL of 0.1 N ammonium acetate buffer

(pH 5.5) and added to the DOTA-RGD solution (about 2−5 μg in 100 μL of 0.1 N ammonium acetate buffer). The reaction mixture was incubated at 45 °C for 45 min. The radiochemical yield was determined by radio-TLC and HPLC. ^{64}Cu-DOTA-RGD was then purified by semipreparative HPLC, and the radioactive peak containing the desired product was collected. After removal of the solvent by rotary evaporation, the residue was reconstituted in 500−800 μL of PBS and passed through a 0.22 μm Millipore filter into a sterile multidose vial for use in the following experiments.

Determination of log *P* Value. The partition coefficient value was expressed as log *P*. log *P* of ^{64}Cu-AmBaSar-RGD was determined by measuring the distribution of radioactivity in 1-octanol and PBS. A 5 μL sample of ^{64}Cu-AmBaSar-RGD in PBS was added to a vial containing 1 mL each of 1-octanol and PBS. After vigorously vortexing for 10 min, the vial was centrifuged for 5 min to ensure the complete separation of layers. Then, 3 × 10 μL of each layer was pipetted into other test tubes, and radioactivity was measured using a gamma counter (Perkin-Elmer Packard Cobra). The measurement was repeated three times, and log *P* values were calculated according to a known formula.

***In Vitro* Stability Assay.** The *in vitro* stability of ^{64}Cu-AmBaSar-RGD and ^{64}Cu-DOTA-RGD was studied at different time points. Briefly, 3.7 MBq of ^{64}Cu-AmBaSar-RGD and ^{64}Cu-DOTA-RGD was pipetted into 1 mL of PBS, fetal bovine serum (FBS), and mouse serum, respectively. After incubation at 37 °C for 3, 18, and 24 h, an aliquot of the mixture was removed from the PBS solution and the radiochemical purity was determined with HPLC. For the solution of FBS and mouse serum, the aliquots were added to 100 μL of PBS with 50% TFA. After centrifugation, the upper solution was taken and filtered for HPLC analysis.

Integrin Receptor Binding Assay and Cell Uptake Study. U87MG human glioblastoma cell line (integrin $\alpha_v\beta_3$-positive) was obtained from the American Type Culture Collection (ATCC, Manassas, VA) and maintained under standard conditions according to ATCC as follows: the U87MG glioma cells were grown in Gibco's Dulbecco's medium supplemented with 10% fetal bovine serum (FBS), 100 IU/mL penicillin, and 100 μg/mL streptomycin (Invitrogen Co, Carlsbad, CA), at 37 °C in humidified atmosphere containing 5% CO_2. The U87MG glioma cells were grown in culture until sufficient cells were available.

The *in vitro* integrin-binding affinity and specificity of AmBaSar-RGD and RGD were assessed via competitive cell binding assays using ^{125}I-echistatin as the integrin $\alpha_v\beta_3$-specific radioligand by a minor modification of a method previously described (*26, 27*). In detail, U87MG cells were harvested, washed three times with PBS, and resuspended (2 × 10^6 cells/mL) in the binding buffer. Filter multiscreen DV plates (96-well, pore size, 0.65 μm, Millipore) were seeded with 10^5 cells and incubated with ^{125}I-echistatin (0.74 kBq/well) in the presence of increasing concentrations of different RGD peptide analogues (0−1,000 nmol/L). The total incubation volume was adjusted to 200 μL. After the cells were incubated for 2 h at room temperature, the plates were filtered through a multiscreen vacuum manifold and washed three times with binding buffer. The hydrophilic polyvinylidenedifluoride (PVDF) filters were collected, and the radioactivity was determined using a gamma counter. The best-fit 50% inhibitory concentration (IC_{50}) values for U87MG cells were calculated by fitting the data with nonlinear regression using GraphPad Prism (GraphPad Software, Inc.). Experiments were performed on triplicate samples.

The cell uptake study was performed as described with some modifications (*25*). Cells were incubated with ^{64}Cu-AmBaSar-RGD (37 kBq/well) or ^{64}Cu-DOTA-RGD at 37 °C for 30 min, 60 min, and 120 min. The blocking experiment was performed by incubating U87MG cells with ^{64}Cu-AmBaSar-RGD (37 kBq/well) in the presence of 2 μg of c(RGDyK). The tumor cells were then washed three times with chilled PBS and harvested by 0.1 N NaOH solution containing 0.5% sodium dodecyl sulfate (SDS). The cell suspensions were collected and measured in a gamma counter.

Animal Model. Athymic nude mice (about 10−20 weeks old, with a body weight of 25−35 g) were obtained from Harlan (Charles River, MA). All animal experiments were performed according to a protocol approved by the University of Southern California Institutional Animal Care and Use Committee. The U87MG human glioma xenograft model was generated by a subcutaneous injection of 5 × 10^6 U87MG human glioma cells into the front flank of athymic nude mice. The tumors were allowed to grow 3−5 weeks until 200−500 mm^3 in volume. Tumor growth was followed by caliper measurements of the perpendicular dimensions.

MicroPET Imaging and Blocking Experiment. MicroPET scans and imaging analysis were performed using a rodent scanner (microPET R4; Siemens Medical Solutions) as previously reported (*26*). About 11.1 MBq of ^{64}Cu-AmBaSar-RGD or ^{64}Cu-DOTA-RGD was intravenously injected into each mouse under isoflurane anesthesia. Ten minute static scans were acquired at 1, 2, 4, and 20 h post-injection. The images were reconstructed by a 2-dimensional ordered-subsets expectation maximum (OSEM) algorithm. For each microPET scan, regions of interest were drawn over the tumor, normal tissue, and major organs on the decay-corrected whole-body coronal images. The radioactivity concentration (accumulation) within the tumor, muscle, liver, and kidneys were obtained from the mean value within the multiple regions of interest and then converted to % ID/g. For the receptor blocking experiment, mice bearing U87MG tumors were scanned (10 min static) at the 2 h time point after the coinjection of 11.1 MBq of ^{64}Cu-AmBaSar-RGD or ^{64}Cu-DOTA-RGD with 10 mg/kg c(RGDyK) per mouse.

Biodistribution Studies. The U87MG tumor bearing nude mice (n = 3) were injected with 0.37 MBq of ^{64}Cu-AmBaSar-RGD or ^{64}Cu-DOTA-RGD to evaluate the biodistribution of these tracers. All mice were sacrificed and dissected at 20 h after the injection of the tracers. Blood, U87MG tumor, major organs, and tissues were collected and weighed wet. The radioactivity in the tissues was measured using a gamma counter. The results were presented as the percentage injected dose per gram of tissue (% ID/g). For each mouse, the radioactivity of the tissue samples was calibrated against a known aliquot of the injected activity. The mean uptake (% ID/g) for each group of animals was calculated with standard deviations.

Metabolic Stability. The metabolic stabilities of ^{64}Cu-AmBaSar-RGD and ^{64}Cu-DOTA-RGD were evaluated in an athymic nude mouse bearing a U87MG tumor. Sixty minutes after the intravenous injection of 11.1 MBq of ^{64}Cu-AmBaSar-RGD or ^{64}Cu-DOTA-RGD, the mouse was sacrificed, and the relevant organs were harvested. The blood was collected immediately and centrifuged for 5 min at 14,000 rpm. Then, 50% TFA in 100 μL of PBS was added to the upper serum solution, followed by mixing and centrifugation for 5 min. The upper solution was then taken and injected for HPLC analysis. The liver, kidneys, and tumor were homogenized using a homogenizer, suspended in 1 mL of PBS buffer, and then centrifuged for 5 min at 14,000 rpm. For each sample, after the removal of the supernatant, 50% TFA in 100 μL PBS was added to the solution, followed by mixing and centrifugation for 5 min. The upper solution was then taken and injected for HPLC analysis. The eluent was collected with a fraction collector (1.5 min/fraction), and the radioactivity of each fraction was measured with a gamma counter.

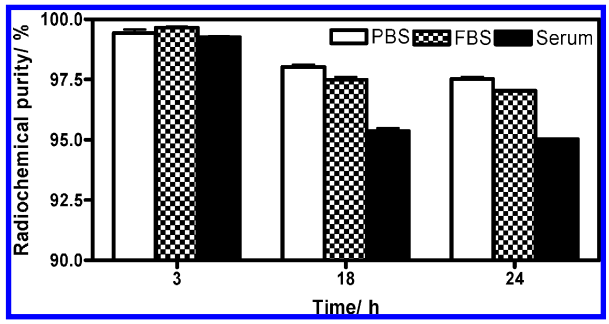

Figure 2. *In vitro* stability of ^{64}Cu-AmBaSar-RGD in PBS (pH 7.4), FBS, and mouse serum for incubation under 37 °C for 3, 18, and 24 h.

Statistical Analysis. Quantitative data were expressed as the mean ± SD. Means were compared using one-way ANOVA and Student'S *t* test. *P* values <0.05 were considered statistically significant.

RESULTS

Chemistry and Radiolabeling. The identity of AmBaSar-RGD and DOTA-RGD conjugates was confirmed by HPLC and mass spectrometry as previously reported (*15, 23*). The AmBaSar-RGD conjugate was obtained in about 80% yield after HPLC purification for both aqueous and organic phase procedures. The ^{64}Cu-labeling (n = 7) was achieved in more than 95% decay-corrected yield for ^{64}Cu-AmBaSar-RGD with a radiochemical purity of >99% and 80% radiochemical yield for ^{64}Cu-DOTA-RGD with a radiochemical purity >98%. ^{64}Cu-AmBaSar-RGD and ^{64}Cu-DOTA-RGD were analyzed and purified by HPLC. The HPLC retention times of ^{64}Cu-AmBaSar-RGD and ^{64}Cu-DOTA-RGD were 26.5 and 21.5 min, respectively, under the analytical conditions. For radio-TLC analysis, the free $^{64}Cu^{2+}$ remained at the origin of the TLC plate, while the R_f values of ^{64}Cu-DOTA-RGD and ^{64}Cu-AmBaSar-RGD were about 0.8−1.0. The specific activity of ^{64}Cu-DOTA-RGD and ^{64}Cu-AmBaSar-RGD was estimated to be about 10.1−22.2 GBq/μmol. Both tracers were used immediately after the formulation.

log *P* Value and *in Vitro* Stability. The octanol/water partition coefficients (log *P*) for ^{64}Cu-AmBaSar-RGD and ^{64}Cu-DOTA-RGD were −2.44 ± 0.12 and −2.80 ± 0.04, respectively (*23*), which demonstrated that both tracers are rather hydrophilic. The *in vitro* stability of ^{64}Cu-AmBaSar-RGD was also studied in PBS (pH 7.4), FBS, and mouse serum for different time intervals (3, 18, and 24 h) at physiological temperature of 37 °C. The stability was presented as the percentage of intact ^{64}Cu-AmBaSar-RGD on the basis of the HPLC analysis, and the results are shown in Figure 2. After 24 h of incubation, more than 97% of ^{64}Cu-AmBaSar-RGD remained intact in the PBS and FBS, and more than 95% of ^{64}Cu-AmBaSar-RGD remained intact in mouse serum. We also found that ^{64}Cu-DOTA-RGD demonstrated similar stability results *in vitro* under the above experimental conditions (data not shown).

***In Vitro* Cell Binding Affinity and Uptake.** We compared the receptor-binding affinity of AmBaSar-RGD and c(RGDyK) using a competitive cell-binding assay (Figure 3A). All peptides inhibited the binding of ^{125}I-echistatin to $\alpha_v\beta_3$ integrin-positive U87MG cells in a dose-dependent manner. The IC_{50} value for AmBaSar-RGD (53.26 ± 0.51 nmol/L) was comparable to that of c(RGDyK) (36.55 ± 0.65 nmol/L). These results had shown that chelator (such as AmBaSar or DOTA) conjugation had a minimal effect on the receptor-binding avidity (*27*).

The cell uptake study of ^{64}Cu-AmBaSar-RGD or ^{64}Cu-DOTA-RGD was performed on U87MG tumor cells, and the cell uptake was expressed as radioactivity (cpm) per 10^6 cells after decay correction as shown in Figure 3B. The cell uptake study revealed that both ^{64}Cu-AmBaSar-RGD and ^{64}Cu-DOTA-RGD could bind to U87MG tumor cells, but relatively low amounts of activity (only about 0.1−0.4% was internalized). However, this binding could be efficiently blocked by an excess amount of cold c(RGDyK) peptide, which demonstrated the binding specificity of the radiolabeled ligands.

MicroPET Imaging. The tumor-targeting efficacy and biodistribution patterns of ^{64}Cu-AmBaSar-RGD and ^{64}Cu-DOTA-RGD were evaluated in nude mice bearing U87MG human glioma xenograft tumors (n = 3) at multiple time points (1, 2, 4, and 20 h) with static microPET scans. Representative decay-corrected coronal images at different time points were shown in Figure 4A. The U87MG tumors were clearly visualized with high tumor-to-background contrast for both tracers. The uptake of ^{64}Cu-AmBaSar-RGD in U87MG tumors was 2.04 ± 0.14, 1.85 ± 0.16, 1.87 ± 0.11, and 0.97 ± 0.05% ID/g at 1, 2, 4, and 20 h p.i., respectively. ^{64}Cu-DOTA-RGD demonstrated similar tumor uptake with the value of 2.03 ± 0.10, 1.97 ± 0.05, 1.88 ± 0.29, and 0.88 ± 0.07% ID/g at the above time points, respectively (Figure 4B). However, the biodistribution patterns of ^{64}Cu-AmBaSar-RGD and ^{64}Cu-DOTA-RGD were significantly different, especially in the kidneys and liver. The renal uptake of ^{64}Cu-AmBaSar-RGD were 2.83 ± 0.77, 2.68 ± 0.55, 2.49 ± 0.50, and 1.43 ± 0.35% ID/g at 1, 2, 4, and 20 h p.i., respectively, while the corresponding uptake for ^{64}Cu-DOTA-RGD was 1.52 ± 0.46, 1.33 ± 0.23, 1.55 ± 0.61, and 1.58 ± 0.13% ID/g, respectively. This was lower than that of ^{64}Cu-AmBaSar-RGD from 1 to 4 h, and reached comparable levels at the 20 h time point. The liver uptake for ^{64}Cu-AmBaSar-RGD was 0.89 ± 0.13, 0.76 ± 0.13, 0.75 ± 0.14, and 0.64 ± 0.06% ID/g at 1, 2, 4, and 20 h p.i.. The corresponding uptake value for ^{64}Cu-DOTA-RGD was 2.28 ±

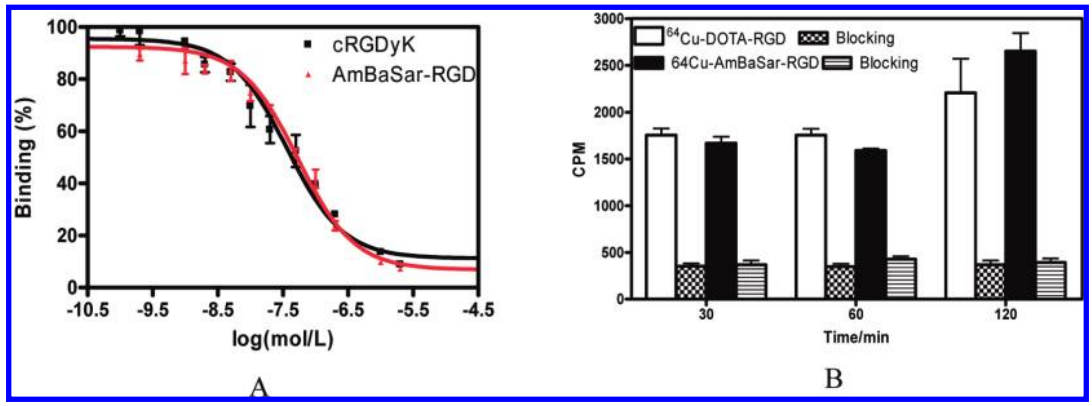

Figure 3. *In vitro* cell integrin receptor binding assay and cell uptake study. (A) *In vitro* inhibition of ^{125}I-echistatin binding to integrin on U87MG cells by c(RGDyK), AmBaSar-RGD, and DOTA-RGD; (B) U87MG cell uptake of ^{64}Cu-AmBaSar-RGD and ^{64}Cu-DOTA-RGD at 0.5, 1, and 2 h in the absence/presence of an excess amount of c(RGDyK) peptide.

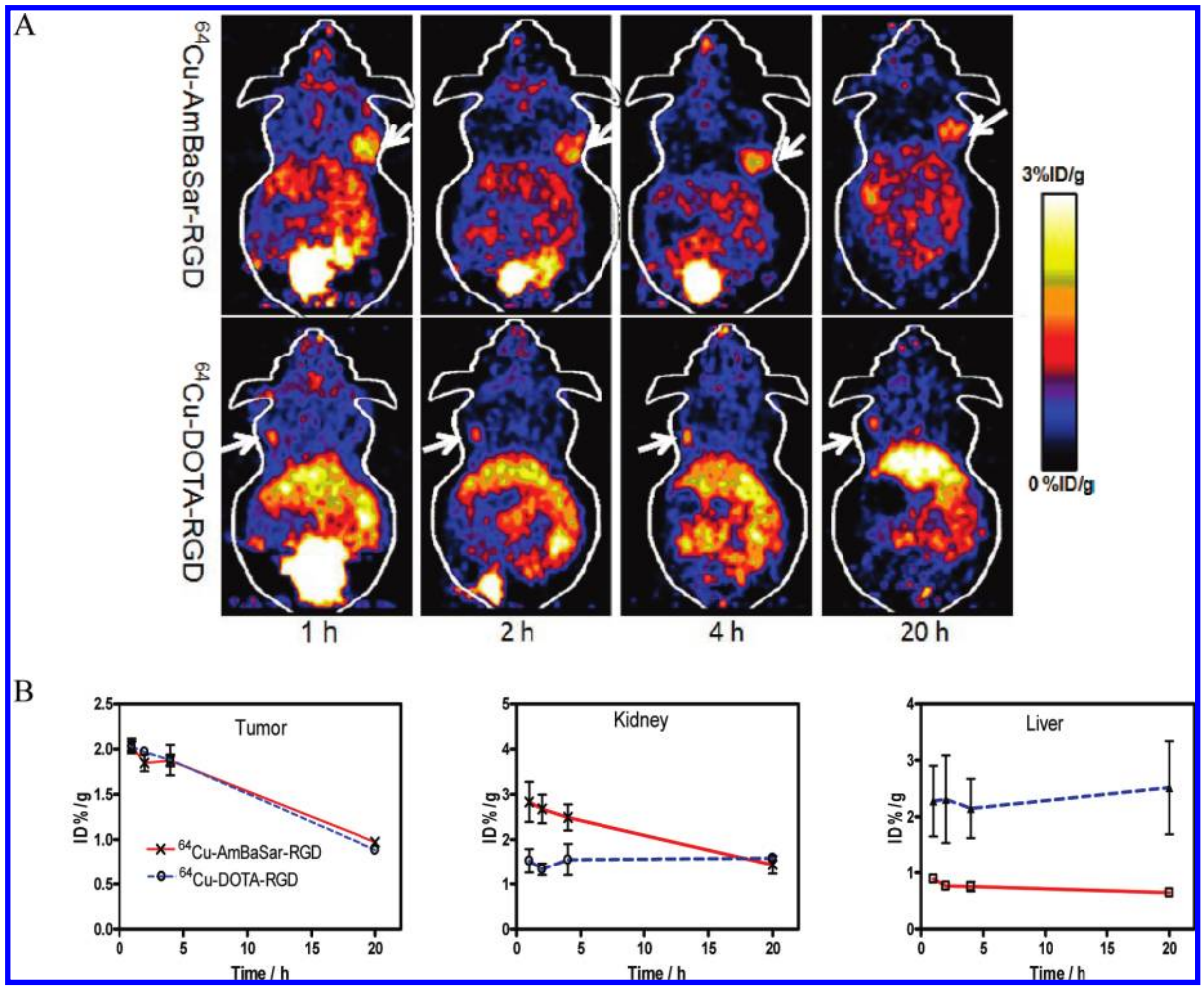

Figure 4. MicroPET study of U87MG tumor-bearing mice. (A) Coronal images of nude mice bearing the U87MG tumor at 1, 2, 4, and 20 h p.i. of ^{64}Cu-AmbaSar-RGD and ^{64}Cu-DOTA-RGD; (B) time activity curves of ^{64}Cu-AmBaSar-RGD and ^{64}Cu-DOTA-RGD in the U87MG tumor, liver, and kidneys ($n = 3$). Tumors are indicated by arrows.

1.08, 2.31 ± 1.34, 2.15 ± 0.90, and 2.52 ± 1.43% ID/g, respectively, which were significantly higher than those of ^{64}Cu-AmBaSar-RGD at all time points.

Blocking Experiment. The integrin $\alpha_v\beta_3$ receptor specificity of ^{64}Cu-AmBaSar-RGD was confirmed by a blocking experiment where the tracers were coinjected with the c(RGDyK) peptide (10 mg/kg). As can be seen from Figure 5, the U87MG tumor uptake in the presence of nonradiolabeled c(RGDyK) peptide (0.09 ± 0.03% ID/g) is significantly lower than that without c(RGDyK) peptide blocking (1.85 ± 0.16% ID/g) ($P < 0.05$) at 2 h p.i. The uptake of ^{64}Cu-AmBaSar-RGD in other organs (heart, intestine, kidneys, lungs, liver, and spleen) was also significantly decreased, which correlates well with previous references (*23*). Similarly, the integrin $\alpha_v\beta_3$ specificity of^{64}Cu-DOTA-RGD was confirmed by blocking experiments (Figure 5).

Biodistribution Studies. To validate the accuracy of small animal PET quantification, we also performed a biodistribution experiment by using the direct tissue sampling technique. The data shown as the percentage administered activity (injected dose) per gram of tissue (% ID/g) in Figure 6A. Both ^{64}Cu-AmBaSar-RGD and ^{64}Cu-DOTA-RGD mainly accumulated in the kidneys, liver, stomach, intestine, and tumor. After 20 h p.i., the kidneys and liver uptake reached 1.51 ± 0.27 and 0.55 ± 0.06% ID/g for ^{64}Cu-AmBaSar-RGD and 0.98 ± 0.40 and 2.16 ± 0.85% ID/g for ^{64}Cu-DOTA-RGD, respectively. This difference was consistent with the excretion pattern from the microPET imaging results. On the basis of the biodistribution results, we also calculated the contrast of the tumor to main organs, which is shown in Figure 6B. For ^{64}Cu-AmBaSar-RGD, the ratio of tumor uptake to muscle, heart, lung, liver, and kidney uptake was 14.20 ± 3.84, 7.33 ± 1.55, 3.34 ± 0.70, 1.18 ± 0.05, and 0.43 ± 0.06, respectively, while the corresponding values for ^{64}Cu-DOTA-RGD were 5.97 ± 2.25, 1.78 ± 0.37, 1.27 ± 0.37, 0.33 ± 0.09, and 0.66 ± 0.04, respectively.

Metabolic Stability of ^{64}Cu-AmBaSar-RGD and ^{64}Cu-DOTA-RGD. The metabolic stability of ^{64}Cu-AmBaSar-RGD and ^{64}Cu-DOTA-RGD were determined in mouse blood and in liver, kidney, and tumor homogenates at 1 h after the intravenous injection of the radiotracer into a U87MG tumor-bearing mouse according to the literature procedures (*28, 29*). The radioactivity of each sample was analyzed by HPLC, and the representative radio-HPLC profiles were shown in Figure 7. There was only one major radiolabeled metabolite with a retention time between 3.0 to 6.0 min. It has been well demonstrated that the cylic-RGDyk peptide is stable *in vivo*. Therefore, it is highly possible that this solvent front peak corresponds to free Cu. Nonetheless, its identity needs to be confirmed in our future studies. The amount of intact tracer in the blood, tumor, liver, and kidneys were approximately 88%, 95%, 98%, and 98% for ^{64}Cu-AmBaSar-RGD and 38%, 87%, 34%, and 74% for ^{64}Cu-DOTA-RGD at 1 h post-injection, respectively.

DISCUSSION

The established BFC DOTA is the most widely used Cu chelation ligand for molecular imaging and radiotherapy (*4, 7, 30*). DOTA has been conjugated to various macromolecules includ-

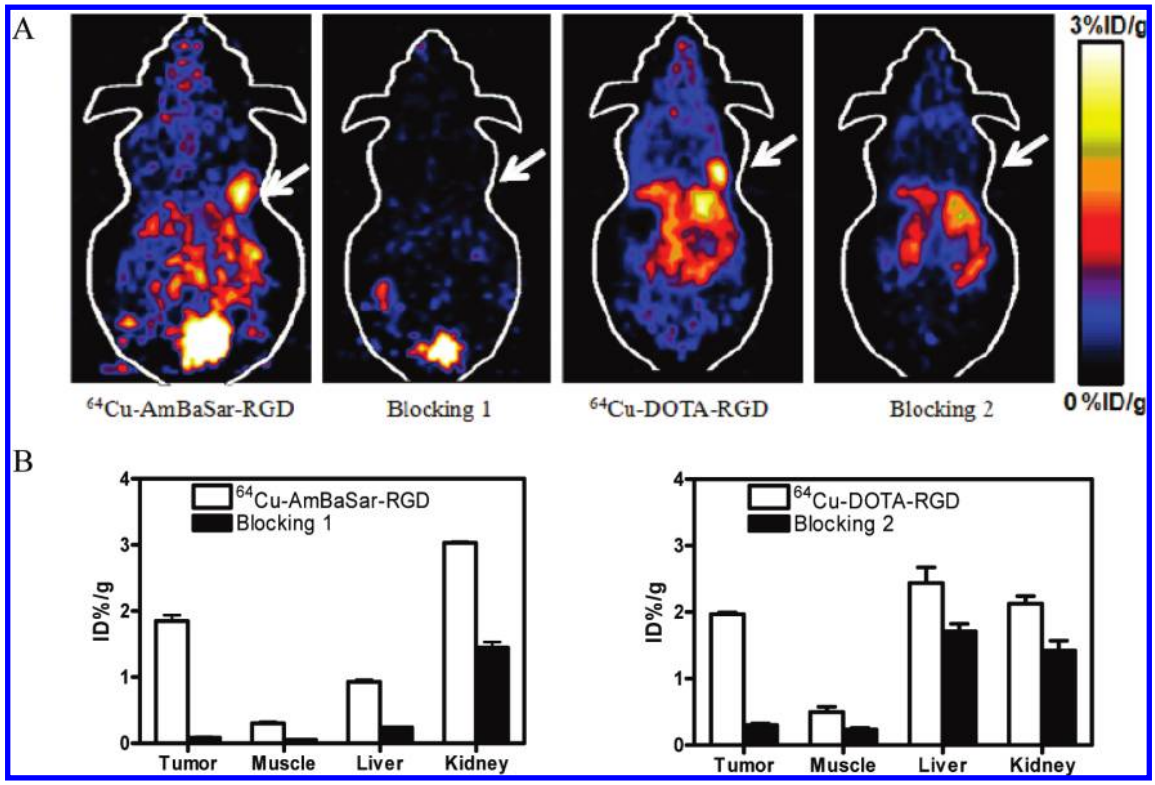

Figure 5. MicroPET imaging of ^{64}Cu-AmBaSar-RGD and ^{64}Cu-DOTA-RGD on the U87MG xenograft mouse model at 2 h p.i. with/without a blocking dose of c(RGDyK) peptide: (A) microPET coronal images. (B) Quantitative analyses of microPET imaging of the U87MG tumor, muscle, liver, and kidneys ($n = 3$). Arrows indicate the tumor positions.

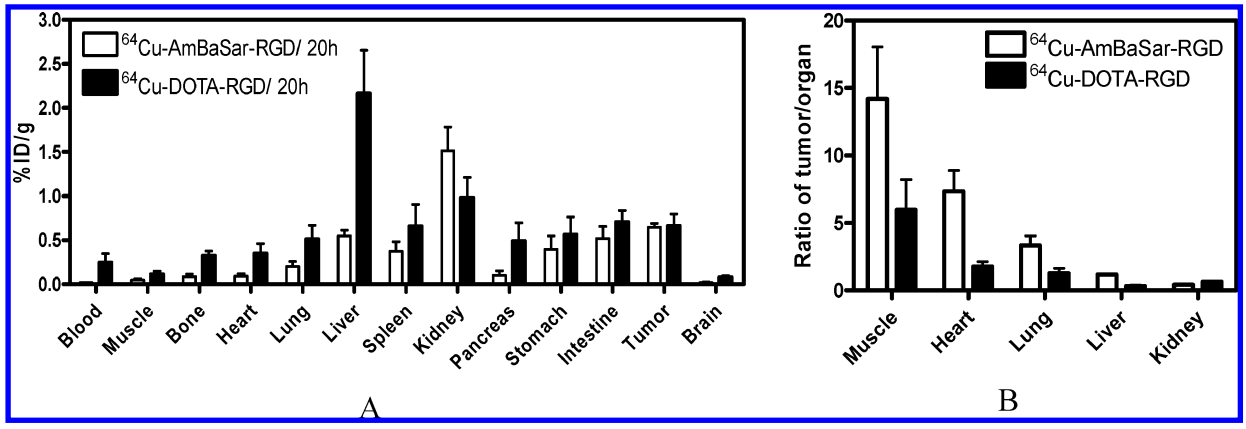

Figure 6. (A) Biodistribution data for ^{64}Cu-AmBaSar-RGD and ^{64}Cu-DOTA-RGD in mice bearing U87MG glioma xenografts (mean ± SD, $n = 3$) at 20 h p.i.; (B) the ratios of tumor to main organ uptake of ^{64}Cu-AmBaSar-RGD and ^{64}Cu-DOTA-RGD.

ing proteins (*31*), antibodies (*32*), peptides (*30*), as well as nanoparticles to track their distributions *in vivo* (*33, 34*). However, under physiological conditions, Cu may be removed from the Cu-DOTA complex and transferred to copper-binding proteins. The significant loss of Cu from the conjugate could lead to high uptake in the liver and fail to reflect the real distribution of the macromolecules. Therefore, the limited stability of the copper chelate *in vivo* has hindered its further applications (*5*). For example, although we have demonstrated that ^{64}Cu-DOTA-RGD could be a suitable tracer for PET imaging of integrin $\alpha_v\beta_3$ expression in breast cancer (*23*), unfavorable hepatobiliary excretion was also observed due to $^{64}Cu^{2+}$ dissociation from the DOTA-RGD conjugate *in vivo*. Recently, we have developed a new cage-like BFC AmBaSar for $^{64}Cu^{2+}$ labeling and demonstrated that this ^{64}Cu-complexing moiety is a superior ligand for imaging application and targeted radiotherapy due to its improved Cu-chelation stability compared with that of DOTA (*16*). We also reported the synthesis of a new PET tracer ^{64}Cu-AmBaSar-RGD that could be possibly used for imaging integrin $\alpha_v\beta_3$ expression (*15*). The objective of this study is to evaluate the $^{64}Cu^{2+}$ labeling and imaging ability of AmBaSar-RGD conjugates and compare the results with the established chelator DOTA using the DOTA-RGD peptide as the standard compound. These studies have demonstrated that ^{64}Cu-AmBaSar-RGD and ^{64}Cu-DOTA-RGD have comparable *in vitro* stability, lipophilicity, and tumor uptake. However, ^{64}Cu-AmBaSar-RGD did demonstrate improved *in vivo* stability and biodistribution pattern compared with those of ^{64}Cu-DOTA-RGD.

From the chemistry point of view, there were no obvious differences between the AmBaSar and DOTA conjugation to the c(RGDyK) peptide. Both chelators used a carboxylate group to directly conjugate with the lysine amine in the c(RGDyK) peptide in high yield. However, for radiochemistry, the $^{64}Cu^{2+}$ labeling condition of AmBaSar-RGD was more favorable, and the ^{64}Cu-AmBaSar-RGD could be obtained with higher radiochemical yield (≥95%) and purity (≥99%) under mild conditions (pH 5.0−5.5, 23−37 °C) in less than 30 min, compared

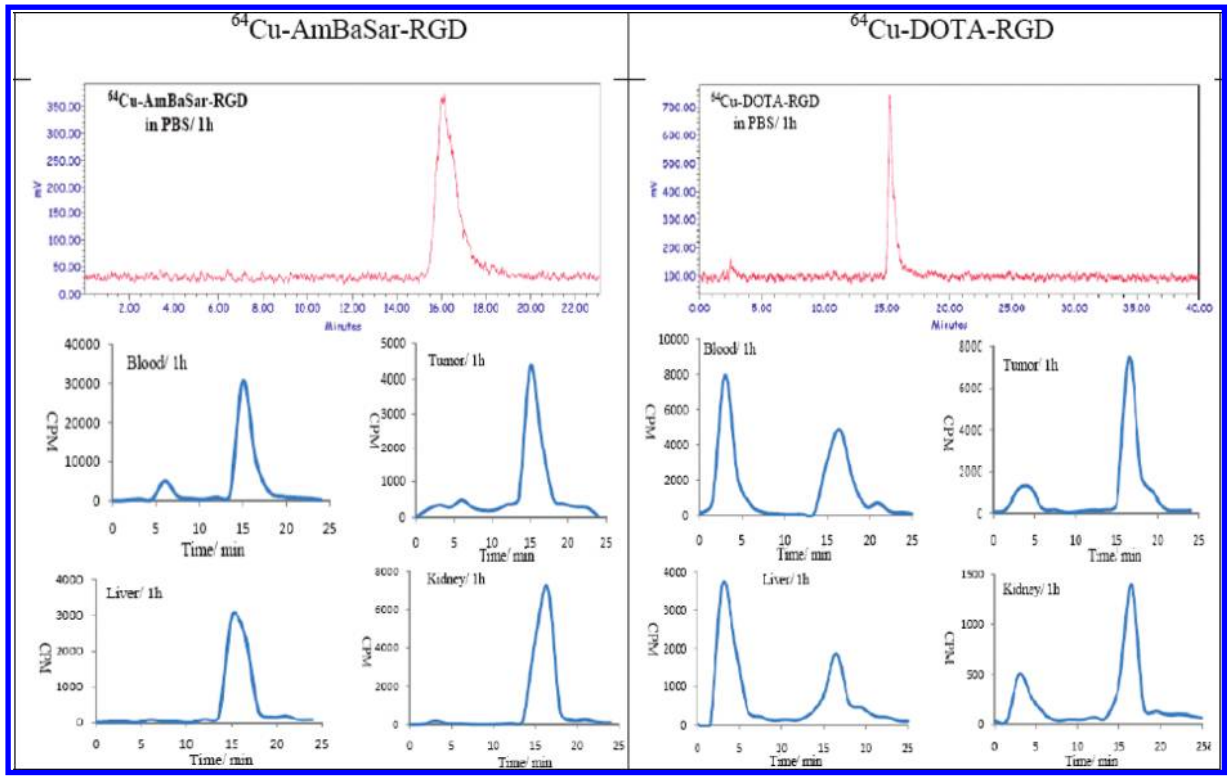

Figure 7. Metabolic stability of ^{64}Cu-AmBaSar-RGD and ^{64}Cu-DOTA-RGD in the mouse blood sample and in the liver, kidney, and U87MG tumor homogenates at 1 h post-injection. The HPLC profiles of pure ^{64}Cu-AmBaSar-RGD and ^{64}Cu-DOTA-RGD (standard) are also shown.

with 90% radiochemical yield for ^{64}Cu-DOTA-RGD after incubation at 45 °C for 45 min.

Under *in vitro* conditions, both ^{64}Cu-AmBaSar-RGD and ^{64}Cu-DOTA-RGD were very stable in PBS, FBS, and mouse serum solutions at physiological temperature. The log *P* value is a very useful parameter that can be used to understand the behavior of drug molecules and predict the distribution of a drug compound in a biological system in combination with other parameters (*35*). The log *P* values of ^{64}Cu-AmBaSar-RGD and ^{64}Cu-DOTA-RGD indicated that both tracers are rather hydrophilic and that they should show rapid blood clearance and preferential renal excretion if the Cu-chelation is stable *in vivo*. However, compared with ^{64}Cu-AmBaSar-RGD, ^{64}Cu-DOTA-RGD had significantly higher liver uptake (∼2−3 times) on the basis of the microPET imaging and biodistrbution studies, which indicated that ^{64}Cu-DOTA-RGD is less stable than ^{64}Cu-AmBaSar-RGD *in vivo*. In microPET studies, the U87MG tumor uptake of ^{64}Cu-AmBaSar-RGD and ^{64}Cu-DOTA-RGD were comparable at selected time points, and the binding specificity was proven by the blocking experiment. The biodistribution study was consistent with the microPET studies. Similar tumor uptake of both tracers may be attributed to their comparable hydrophilicity and the minimal impact of chelators on the integrin binding affinity of c(RGDyK) peptides (*36*). ^{64}Cu-AmBaSar-RGD cleared rapidly from the blood and predominantly through the kidneys, and ^{64}Cu-DOTA-RGD mainly cleared through both kidneys and liver. This difference might be because the Cu-chelation in ^{64}Cu-AmBaSar-RGD is more stable *in vivo* compared with that in ^{64}Cu-DOTA-RGD, which would result in reduced nonspecific binding. To further confirm this statement, we also studied the metabolic stability of ^{64}Cu-AmBaSar-RGD and ^{64}Cu-DOTA-RGD in blood, liver, kidneys, and tumors in nude mice bearing U87MG glioma xenografts after 1 h p.i. Our study clearly demonstrated that the amount of intact ^{64}Cu-AmBaSar-RGD was much higher than that of ^{64}Cu-DOTA-RGD in blood, tumor, liver, and kidneys. To the best of our knowledge, this is the first study that directly demonstrates that a Sar-type chelator, such as AmBaSar, forms a more stable Cu complex *in vivo* than the established chelator DOTA through direct comparison of their metabolic stability. We would also like to point out that the rapid renal clearance of ^{64}Cu-AmBaSar-RGD, as opposed to the mixed renal and hepatic clearance of ^{64}Cu-DOTA-RGD is preferred as it will provide better somatic contrast from the imaging perspective and potentially reduce radiation exposure.

CONCLUSIONS

^{64}Cu-AmBaSar-RGD was obtained in high yield under mild conditions for PET imaging of integrin $\alpha_v\beta_3$ expression. This tracer exhibited good tumor-targeting efficacy, excellent metabolic stability, as well as favorable *in vivo* pharmacokinetics. *In vitro* and *in vivo* evaluation of the ^{64}Cu-AmBaSar-RGD has demonstrated its improved *in vivo* Cu-chelation stability compared with that of the established tracer ^{64}Cu-DOTA-RGD. The AmBaSar chelator will also have a general application for ^{64}Cu labeling of various bioactive molecules in high radiochemical yield and high *in vivo* Cu-chelation stability for future PET applications.

ACKNOWLEDGMENT

This work was supported partially by research grant DE-SC0002353 from the Department of Energy, the USC Department of Radiology, and the Provost's Biomedical Imaging Science Initiative.

LITERATURE CITED

(1) Voss, S. D., Smith, S. V., DiBartolo, N., McIntosh, L. J., Cyr, E. M., Bonab, A. A., Dearling, J. L., Carter, E. A., Fischman, A. J., Treves, S. T., Gillies, S. D., Sargeson, A. M., Huston, J. S., and Packard, A. B. (2007) Positron emission tomography (PET) imaging of neuroblastoma and melanoma with ^{64}Cu-SarAr immunoconjugates. *Proc. Natl. Acad. Sci. U.S.A. 104*, 17489–17493.

(2) Shokeen, M., and Anderson, C. J. (2009) Molecular imaging of cancer with copper-64 radiopharmaceuticals and positron emission tomography (PET). *Acc. Chem. Res. 42*, 832–841.
(3) Eckelman, W. C., Reba, R. C., and Kelloff, G. J. (2008) Targeted imaging: an important biomarker for understanding disease progression in the era of personalized medicine. *Drug Discovery Today 13*, 748–759.
(4) Tanaka, K., and Fukase, K. (2008) PET (positron emission tomography) imaging of biomolecules using metal-DOTA complexes: a new collaborative challenge by chemists, biologists, and physicians for future diagnostics and exploration of in vivo dynamics. *Org. Biomol. Chem. 6*, 815–828.
(5) Wadas, T. J., Wong, E. H., Weisman, G. R., and Anderson, C. J. (2007) Copper chelation chemistry and its role in copper radiopharmaceuticals. *Curr. Pharm. Des 13*, 3–16.
(6) Blower, P. J., Lewis, J. S., and Zweit, J. (1996) Copper radionuclides and radiopharmaceuticals in nuclear medicine. *Nucl. Med. Biol. 23*, 957–980.
(7) Liu, S. (2008) Bifunctional coupling agents for radiolabeling of biomolecules and target-specific delivery of metallic radionuclides. *Adv. Drug Delivery Rev. 60*, 1347–1370.
(8) Smith, S. V. (2004) Molecular imaging with copper-64. *J. Inorg. Biochem 98*, 1874–1901.
(9) Anderson, C. J., Wadas, T. J., Wong, E. H., and Weisman, G. R. (2008) Cross-bridged macrocyclic chelators for stable complexation of copper radionuclides for PET imaging. *Q. J. Nucl. Med. Mol. Imaging 52*, 185–192.
(10) Ferreira, C. L., Yapp, D. T., Lamsa, E., Gleave, M., Bensimon, C., Jurek, P., and Kiefer, G. E. (2008) Evaluation of novel bifunctional chelates for the development of Cu-64-based radiopharmaceuticals. *Nucl. Med. Biol. 35*, 875–882.
(11) Sargeson, A. M. (1996) The potential for the cage complexes in biology. *Coord. Chem. Rev. 151*, 89–114.
(12) Smith, S. V. (2008) Sarar technology for the application of Copper-64 in biology and materials science. *Q. J. Nucl. Med. Mol. Imaging 52*, 193–202.
(13) DiBartolo, N., Sargeson, A. M., Donlevy, T. M., and Smith, S. V. (2001) Synthesis of a new cage ligand, SarAr, and its complexation with selected transition metal ions for potential use in radioimaging. *J. Chem. Soc., Dalton Trans.* , 2303–2309.
(14) DiBartolo, N., Sargeson, A. M., and Smith, S. V. (2006) New^{64}Cu PET imaging agents for personalised medicine and drug development using the hexa-aza cage, SarAr. *Org. Biomol. Chem. 4*, 3350–3357.
(15) Cai, H., Fissekis, J., and Conti, P. S. (2009) Synthesis of a novel bifunctional chelator AmBaSar based on sarcophagine for peptide conjugation and ^{64}Cu radiolabelling. *Dalton Trans.* , 5395–5400.
(16) Cai, H., Li., Z., Huang, C., Park, R., Shahinian, A., and Conti, P. S. (2010) An improved synthesis and biological evaluation of a new caged-like bifunctional chelator 4-((8-amino-3, 6, 10, 13, 16, 19- hexaazabicyclo [6.6.6] icosane-1-ylamino) methyl) benzoic acid (AmBaSar) for ^{64}Cu-radiopharmaceuticals. *Nucl. Med. Biol. 37*, 57–65.
(17) Varner, J. A., and Cheresh, D. A. (1996) Tumor angiogenesis and the role of vascular cell integrin $\alpha_v\beta_3$. *Important Adv. Oncol.* 69–87.
(18) Wadas, T. J., Deng, H., Sprague, J. E., Zheleznyak, A., Weilbaecher, K. N., and Anderson, C. J. (2009) Targeting the $\alpha_v\beta_3$ integrin for small-animal PET/CT of osteolytic bone metastases. *J. Nucl. Med. 50*, 1873–1880.
(19) Cai, W., and Chen, X. (2008) Multimodality molecular imaging of tumor angiogenesis. *J. Nucl. Med. 49* (2), 113S–128S.
(20) Schottelius, M., Laufer, B., Kessler, H., and Wester, H. J. (2009) Ligands for mapping $\alpha_v\beta_3$-integrin expression in vivo. *Acc. Chem. Res. 42*, 969–80.
(21) Liu, S. (2006) Radiolabeled multimeric cyclic RGD peptides as integrin $\alpha_v\beta_3$ targeted radiotracers for tumor imaging. *Mol. Pharmaceutics 3*, 472–487.
(22) Haubner, R., and Wester, H. J. (2004) Radiolabeled tracers for imaging of tumor angiogenesis and evaluation of anti-angiogenic therapies. *Curr. Pharm. Des. 10*, 1439–1455.
(23) Chen, X., Park, R., Tohme, M., Shahinian, A. H., Bading, J. R., and Conti, P. S. (2004) MicroPET and autoradiographic imaging of breast cancer α_v-integrin expression using ^{18}F- and ^{64}Cu-labeled RGD peptide. *Bioconjugate Chem. 15*, 41–49.
(24) Achilefu, S., Bloch, S., Markiewicz, M. A., Zhong, T., Ye, Y., Dorshow, R. B., Chance, B., and Liang, K. (2005) Synergistic effects of light-emitting probes and peptides for targeting and monitoring integrin expression. *Proc. Natl. Acad. Sci. U.S.A. 102*, 7976–7981.
(25) Decristoforo, C., Hernandez Gonzalez, I., Carlsen, J., Rupprich, M., Huisman, M., Virgolini, I., Wester, H. J., and Haubner, R. (2008) ^{68}Ga- and ^{111}In-labelled DOTA-RGD peptides for imaging of $\alpha_v\beta_3$ integrin expression. *Eur. J. Nucl. Med. Mol. Imaging 35*, 1507–1515.
(26) Li, Z., Cai, W., Cao, Q., Chen, K., Wu, Z., He, L., and Chen, X. (2007) ^{64}Cu-labeled tetrameric and octameric RGD peptides for small-animal PET of tumor $\alpha_v\beta_3$ integrin expression. *J. Nucl. Med. 48*, 1162–1171.
(27) Chen, X., Hou, Y., Tohme, M., Park, R., Khankaldyyan, V., Gonzales-Gomez, I., Bading, J. R., Laug, W. E., and Conti, P. S. (2004) Pegylated Arg-Gly-Asp peptide: ^{64}Cu labeling and PET imaging of brain tumor alphavbeta3-integrin expression. *J. Nucl. Med. 45*, 1776–1783.
(28) Juran, S., Walther, M., Stephan, H., Bergmann, R., Steinbach, J., Kraus, W., Emmerling, F., and Comba, P. (2009) Hexadentate bispidine derivatives as versatile bifunctional chelate agents for copper(II) radioisotopes. *Bioconjugate Chem. 20*, 347–359.
(29) Shi, J., Kim, Y. S., Zhai, S., Liu, Z., Chen, X., and Liu, S. (2009) Improving tumor uptake and pharmacokinetics of ^{64}Cu-labeled cyclic RGD peptide dimers with Gly_3 and PEG_4 linkers. *Bioconjugate Chem. 20*, 750–759.
(30) De Leon-Rodriguez, L. M., and Kovacs, Z. (2008) The synthesis and chelation chemistry of DOTA-peptide conjugates. *Bioconjugate Chem. 19*, 391–402.
(31) Wang, H., Chen, K., Cai, W., Li, Z., He, L., Kashefi, A., and Chen, X. (2008) Integrin-targeted imaging and therapy with RGD4C-TNF fusion protein. *Mol. Cancer Ther. 7*, 1044–1053.
(32) Eiblmaier, M., Meyer, L. A., Watson, M. A., Fracasso, P. M., Pike, L. J., and Anderson, C. J. (2008) Correlating EGFR expression with receptor-binding properties and internalization of ^{64}Cu-DOTA-cetuximab in 5 cervical cancer cell lines. *J. Nucl. Med. 49*, 1472–1479.
(33) Jarrett, B. R., Gustafsson, B., Kukis, D. L., and Louie, A. Y. (2008) Synthesis of ^{64}Cu-labeled magnetic nanoparticles for multimodal imaging. *Bioconjugate Chem. 19*, 1496–1504.
(34) Rossin, R., Muro, S., Welch, M. J., Muzykantov, V. R., and Schuster, D. P. (2008) In vivo imaging of ^{64}Cu-labeled polymer nanoparticles targeted to the lung endothelium. *J. Nucl. Med. 49*, 103–111.
(35) Valko, K. (2004) Application of high-performance liquid chromatography based measurements of lipophilicity to model biological distribution. *J. Chromatogr., A 1037*, 299–310.
(36) Wei, L., Ye, Y., Wadas, T. J., Lewis, J. S., Welch, M. J., Achilefu, S., and Anderson, C. J. (2009) ^{64}Cu-labeled CB-TE2A and diamsar-conjugated RGD peptide analogs for targeting angiogenesis: comparison of their biological activity. *Nucl. Med. Biol. 36*, 277–285.

BC900537F